# The Aquarius Scatterometer

## An Active System for Measuring Surface Roughness for Sea-Surface Brightness Temperature Correction

Adam Freedman, Dalia McWatters, Michael Spencer
Jet Propulsion Laboratory, California Institute of Technology
4800 Oak Grove Dr., Pasadena, CA 91109 USA
[Adam.Freedman@jpl.nasa.gov]

***Abstract* – The Aquarius scatterometer is a total-power L-band radar system for estimating ocean surface roughness. Its measurements will enable the removal of wind effects from the Aquarius radiometer ocean-surface brightness temperature measurements being used to retrieve ocean salinity. The Aquarius scatterometer is a relatively simple, low-spatial resolution power-detecting radar, without ranging capability. But to meet its science requirement, it must be very stable, with repeatability on the order of 0.1 dB over several days, and calibrated accuracy to this level over several months. Data from this instrument over land as well as ocean areas will be available for a variety of geophysical applications.**

***Keywords – sea-surface salinity; radar scatterometer; ocean roughness.***

### I. Introduction

Ocean roughness can perturb L-band ocean-surface brightness temperatures by several degrees, and this effect must be removed before ocean salinity can be retrieved from the brightness temperature measurements. The Aquarius Instrument [1] includes a radar scatterometer, co-pointing with the primary radiometer subsystem, to actively estimate ocean roughness and enable this temperature correction. The radar itself is relatively simple in design; the primary technical challenge is its end-to-end system stability.

The scatterometer performance requirements flow from the needed sea-surface brightness temperature accuracy via a model function incorporating roughness, brightness temperature, and radar backscatter as a function of wind speed, wind direction, long-period wave height, incidence angle, and polarization direction. Due to ionospheric Faraday rotation at L-band, the pure co-polarization backscatter signature is not directly measurable; thus, the baseline mode of the scatterometer is a total backscatter power measurement, insensitive to Faraday rotation. (If Faraday rotation can be successfully estimated by the radiometer or by ancillary data, co-pol backscatter may be recoverable.)

### II. Required Performance

In windy conditions, the ocean roughness affects sea-surface brightness the most and yields the strongest backscatter. For winds greater than 15-20 m/s, normalized backscatter can reach levels of –10 dB and higher. The scatterometer measurement itself (excluding errors in the model function and atmospheric propagation) is allocated a root-mean squared (rms) brightness temperature error contribution of 0.12 K. A model function [2,3] including effects of wind speeds, ocean conditions, and incidence angle was used to derive the scatterometer power accuracy requirements needed to meet this brightness temperature goal as a function of ocean backscatter. The requirement results are shown in Fig. 1, together with estimates of the Aquarius scatterometer performance.

At high backscatter levels (high ocean winds), the backscatter must be measured to an accuracy of about 0.1 dB rms. This is a very challenging accuracy level for a radar. It dictates how many independent measurements must be averaged (number of looks needed), the transmit bandwidth and pulse length, and the stability over time of the radar electronics. It is not dependent on the signal-to-noise ratio (SNR), as the strong return signal is much larger than the system noise. At low winds speeds, the ocean roughness has a smaller effect on ocean brightness temperature. Although the uncertainty on the backscatter estimate can be larger (>0.5 dB), the required SNR dictates radar transmit power, antenna gain, noise figure, etc.

### III. Radar Characteristics

The Aquarius scatterometer radar and observing parameters are summarized in Tables I and II. Since the Aquarius instrument consists of three separate feeds using

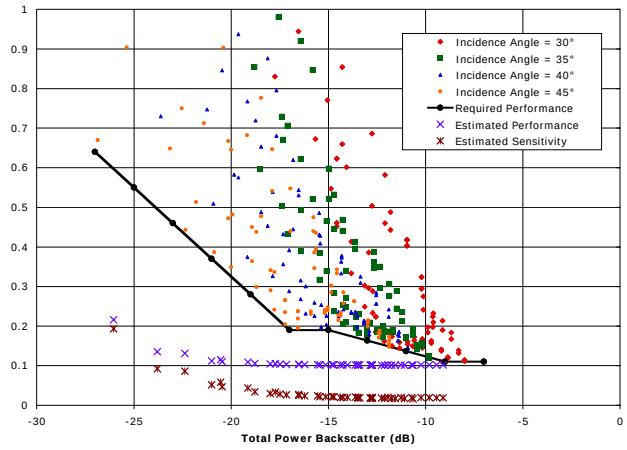


Figure 1. Scatterometer accuracy required for 0.12 K $T_B$ uncertainty compared to the Aquarius scatterometer's expected performance.

The research carried out in this paper was performed by the Jet Propulsion Laboratory under a contract with the National Aeronautics and Space Administration.

one offset-parabolic reflector, three beams are generated forming a swath on the ground about 370 km wide, as illustrated in Fig. 2. Note that a number of the key scatterometer parameters are dictated by the need to coexist and share an antenna with the radiometer subsystem. The relatively low pulse repetition frequency (PRF) of 100 Hz, for example, was dictated by the radiometer's need for continuous, several millisecond-long integration periods.

The performance requirements indicated in Fig. 1 represent the total effect of several scatterometer error sources. The largest time-dependent instrument power fluctuations are due to fluctuations in gain; these are continuously estimated through loopback power measurements during the radar transmit interval. Long-term stability, i.e., the instrument drift over hours, days, and even months, can contribute no more than 0.1 dB of rms error. Over short time scales, from the orbit period of 1.6 hours up to the ground repeat-track interval of 7 days, this stability is to be ensured via tight thermal control of the sensitive radio-frequency (RF) electronics. Over longer time scales, both thermal control and temperature-dependent calibration correction will ensure that drift errors do not exceed 0.1 dB rms. Precise altitude and attitude control will ensure accurate range corrections.

TABLE I. RADAR PARAMETERS COMMON TO ALL BEAMS

| Parameter | Value |
|---|---|
| Nominal Launch and Mission Duration | Spring, 2009, for 3 years |
| Equatorial Altitude (km) | 657 |
| Orbit Inclination (deg) | 98 |
| Orbit Equatorial Crossing | 6:00 PM ascending |
| Ground-track repeat interval | 7 days, 103 orbits |
| Radar Frequency (MHz) | 1260 |
| Transmit/Receive Band Width (MHz) | 4/5 |
| Polarization[a] | HH, HV, VV, VH |
| Pulse Repetition Frequency, PRF (Hz) | 100 |
| No. Measurements Per Second | 5.6 |
| Transmitter Power (W) | 200 - 250 |
| Transmit Pulse Length (ms) | 1 |
| Measurement Integration Time[b] (s) | 6 |
| Dynamic Range (sigma-0) | 0 dB to –40 dB |
| Antenna | 2.5-m offset parabola |
| Feedhorns | 3 feeds, 50 cm diameter |
| Attitude Control/Knowledge (degrees) | 0.5 / 0.1 |

[a] Received power on four channels are summed to create a total power measurement.
[b] Nominal ground-processing averaging time for scatterometer data products.

TABLE II. RADAR PARAMETERS PER BEAM

| Parameter | Inner | Middle | Outer |
|---|---|---|---|
| Look Angle (deg) | 25.9 | 33.9 | 40.3 |
| Azimuth Angle (deg) | 9.7 | -15.3 | 6.5 |
| Incidence Angle (deg) | 28.8 | 37.9 | 45.5 |
| Average 3 dB Beam Width[c] (deg) | 6.5 / 4.7 | 6.7 / 4.8 | 7.1 / 5.1 |
| Peak Gain (dBi) | 28.5 | 28.1 | 27.7 |
| Peak Cross-Pole Gain (dBi) | 6.3 | 8.4 | 10.1 |
| Pulse Integration Time (ms) | 1.8 | 2 | 2.3 |
| Footprint Size (3 dB two-way) | 71 x 58 | 91 x 65 | 122 x 74 |

[c] one-way / two-way 3 dB beam widths.

The other major source of instrument measurement error comes from fading and speckle, which have characteristics akin to thermal noise. These errors average down with longer integration time and a larger number of effective independent "looks". The bandwidth-time product is critical here, and this portion of the error budget (<< 0.1 dB for high SNR situations) dictates the 4 MHz transmit frequency, 1 ms transmit pulse length, and the 6 second final scatterometer data product.

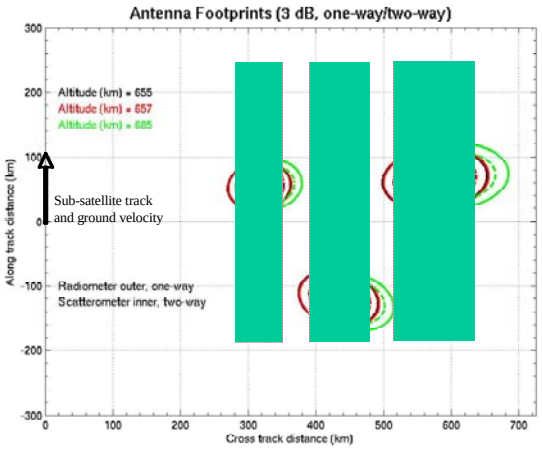


Figure 2. Ground footprints and swaths of the three Aquarius beams relative to the sub-spacecraft location and ground track. The inner, dashed ellipses indicate the two-way 3-dB scatterometer footprints.

These error sources are traditionally broken down using $K_p$, the normalized measurement error:

$$K_{p,TP} = \frac{\sqrt{\mathrm{Var}[\sigma_{TP}]}}{\sigma_{TP}} = \sqrt{K_{pr}^{\ 2} + K_{pc,TP}^{\ 2}} = \sqrt{K_{pr}^2 + \frac{\sum\left[K_{pc}^2(\sigma_i)\times\sigma_i^{\ 2}\right]}{\left(\sum\sigma_i\right)^2}} \quad (1)$$

$K_{pr}$ is the total relative error in knowledge of all parameter values in the radar equation other than ocean backscatter, while $K_{pc}$ is the inherent sensitivity of the measurement to the random effects of fading and thermal noise and is a function of backscatter power and SNR [4],

$$K_{pc,\mathrm{performance}} = \frac{1}{\sqrt{N_p\beta_t\tau_f}}\sqrt{1+\frac{2}{S}\left(\frac{\beta_t\tau_f}{\beta_r\tau_r}\right)+\frac{1}{S^2}\left(\frac{\beta_t\tau_f}{\beta_r\tau_r}\right)\left(1+\frac{\tau_r}{\tau_n}\right)} \quad (2)$$

$$S = \frac{P\tau_t}{\beta_r\tau_r N_0}$$

where the following variables are used in (1) and (2):

$TP$ = Total power quantity
$\sigma_{TP}, \sigma_i$ = Radar backscatter level for TP measurement, or polarimetric channel $i$
$N_p$ = Number of transmit pulses averaged
$\beta_t$ = transmit bandwidth
$\beta_r$ = receive bandwidth
$\tau_t$ = length of transmitted pulse
$\tau_f$ = footprint "fill" time
$\tau_r$ = length of echo receive window ( $\geq \tau_t + \tau_f$ )
$\tau_n$ = length of noise-only receive window
$S$ = signal-to-noise ratio
$P$ = maximum received power
$N_0$ = noise power spectral density

In Fig. 1, the curve marked "Estimated Performance" corresponds to the instrument portion of total-power $K_p$, including $K_{pc}$ and the $K_{pr}$ errors in gain and instrument losses (range and propagation loss errors are not included). The curve marked "Estimated Sensitivity" corresponds to the predicted $K_{pc}$ of the instrument. At high ocean backscatter, the instrument stability is the dominant error source, while at low ocean backscatter, the low SNR dominates.

Since the ionosphere will rotate the polarizations of any transmitted and reflected signal, the Aquarius scatterometer is partially polarimetric. The transmitter alternates between horizontal and vertical polarizations, as does the receiver, in a six-step sequence shown in Fig. 3. A 1 ms transmit event is followed by a 9 ms gap (sufficient for the radiometer integration measurement) within which the echo can be detected. The receive window has a commandable start delay and window length (up to 4 ms). Noise-only measurements are also included in the sequence, which is then repeated for each of the three beams. The total measurement sequence consists of 18 measurements and lasts 0.18 seconds. Note that polarimetric cross-correlations cannot be collected due to the single-string design of the Aquarius scatterometer and its low PRF.

For total power (TP) processing, all co-pol and cross-pol power measurements (HH, HV, VV, VH) are summed, and represent the total ocean backscatter from a set of orthogonal transmit polarizations. This TP sum is independent of Faraday rotation. The strongest ocean return, usually corresponding to the VV backscatter, tends to control the TP magnitude for expected levels of Faraday rotation.

## IV. Radar Design

A block diagram of the Aquarius scatterometer is shown in Fig. 4. The radar consists of a Scatterometer Back End (SBE), Scatterometer Front End (SFE), diplexers, couplers, ortho-mode transducers (OMT), feeds, associated cabling, and the reflector. In addition, a chirp generator and solid-state power amplifier (SSPA) are used to generate the high-power radar transmit signal. Digital data processing is performed external to the Scatterometer subsystem by the Instrument Command and Data Subsystem (ICDS). The ICDS computes average echo power, noise-only power, loopback power, and measures any DC-bias voltage. It will also compute a warning flag for radio-frequency interference (RFI) based on commandable power threshold levels.

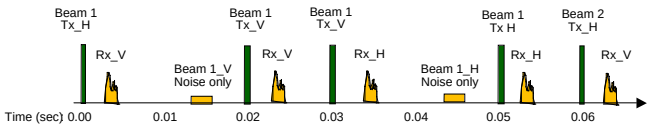


Figure 3. Scatterometer timing sequence. First echo is "HV1": H-pol transmit, V-pol receive, on Beam 1.

A greatly attenuated portion of the transmit signal is routed to the receiver through the loopback path and is used to calibrate drifts in transmit and receive gain. Two loopback attenuators are not part of the actual echo transmit and receive path; thus variations in loss of these two components must be kept very small or removed after the fact via calibration data. Portions of the echo transmit and receive path not part of the loopback also must have very stable losses. The diplexer, coupler, and OMT portions of the Tx/Rx path must already be stable or calibratable to a level an order-of-magnitude greater than the scatterometer requires to meet the radiometer's measurement stability. But the scatterometer relies on a 7-pole switch which must have an extremely stable loss.

Aquarius uses several approaches to meet these tight stability requirements. First, the SFE and SBE will be tightly temperature controlled using an active thermal control system. The system consists of a precise proportional-integral (PID) controller and heater within a thermally insulated zone connected to a radiator plate. This system is expected to maintain the SFE and SBE to within 0.4°C rms over orbit and several-day time scales. (Front-end components such as the diplexer and OMT are within an active thermal control zone with a 0.1°C rms stability requirement.) Second, the SFE and SBE are instrumented with several high-precision temperature sensors which are used to both verify temperature stability and to correct for temperature drifts using component and system loss-temperature curves collected prior to launch. Thus, pre-launch scatterometer calibration is a key part of the instrument design. Third, the ground processing team will use several ground-truth techniques and validation sites to remove slowly-varying post launch biases and drifts. These latter two techniques can remove monotonic, long-period, and seasonal drifts from the scatterometer measurement data, with the objective of detecting true fluctuations in backscatter and brightness temperature over the annual cycle and mission lifetime.

## V. Data Products

The Aquarius scatterometer will return estimates of backscatter power continuously over most of the Earth, including land and ice as well as ocean areas. Although the exact processing sequence has not been finalized, the raw data collected in 0.18 second cycles will be corrected for gain fluctuations using the loopback measurements, corrected for thermal noise using the noise-only measurements, averaged into sub-second bins, combined into the TP measurement product, and averaged to generate a final 6-second scatterometer total-backscatter-power data product. This product will have an along-track spatial

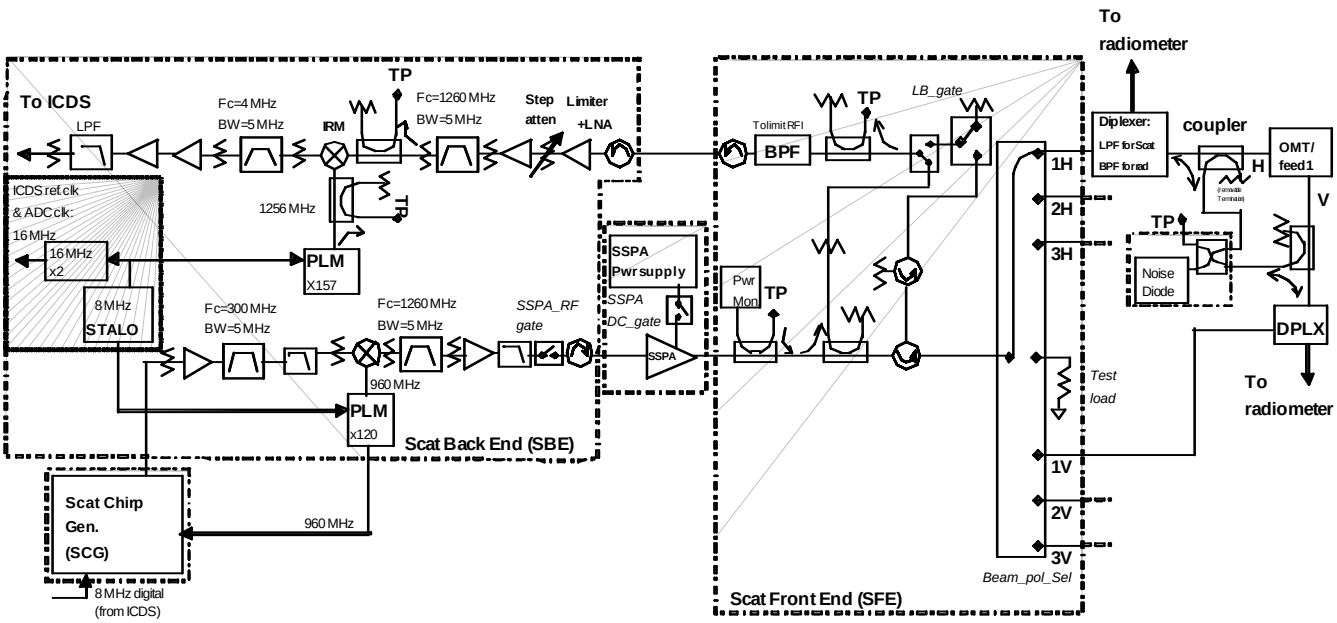


Figure 4. Scatterometer block diagram

resolution of approximately 70 km, and cross-track resolution of about 100 km, depending on the beam. Geophysical corrections will also be applied, including atmospheric propagation corrections, and range (spacecraft altitude and attitude) corrections. The scatterometer will provide flagging of data potentially contaminated with RFI from terrestrial radars.

Ground calibration and ground-truth data will be used to refine an algorithm to convert the measured backscatter into brightness temperature corrections appropriate for the Aquarius radiometer. This is expected to be an active area of Aquarius scatterometer research after launch.

The form and variety of scatterometer data products generated for scientific uses is still under review. The polarimetric data (prior to TP combination), either corrected or uncorrected for Faraday rotation, is a possible intermediate product. The ocean backscatter may be adjusted for wind direction and long-wavelength swells to yield L-band derived wind-generated roughness estimates for comparison with wind speeds estimated by other space-based instruments. The land backscatter data are expected to be useful for soil moisture, freeze-thaw, and snow and ice investigations.

## REFERENCES


[1] S. H. Yueh, W. J. Wilson, W. Edelstein, D. Farra, M. Johnson, F. Pellerano, D. LeVine, and P. Hilderbrand, "Aquarius Instrument Design For Sea Surface Salinity Measurements," *Proceedings IGARSS '03*, pp. 2795-2797, 2003.

[2] S. H. Yueh, W. J. Wilson, and S. Dinardo, "Polarimetric radar remote sensing of ocean surface wind," *IEEE Transactions on Geoscience and Remote Sensing*, vol. 40, pp. 793-800, 2002.

[3] C. Le and S. Yueh, "Long-Wave Slope Impact on L-Band Radar and Radiometer Measurements and Preliminary Incident Angle Selection Requirement." *Eng. Memo 334E.2004.06*, Pasadena, CA: Jet Propulsion Laboratory, 2004.

[4] M. W. Spencer, C. Wu, and D. G. Long, "Improved resolution backscatter measurements with the SeaWinds pencil-beam scatterometer," *IEEE Transactions on Geoscience and Remote Sensing*, vol. 38, pp. 89-104, 2000.